



Bachelor Thesis

Control Allocation of a Tilting Rotor Hexacopter

Author(s):

Elkhatib, Omar

Publication Date:

2017

Permanent Link:

<https://doi.org/10.3929/ethz-b-000224598> →

Rights / License:

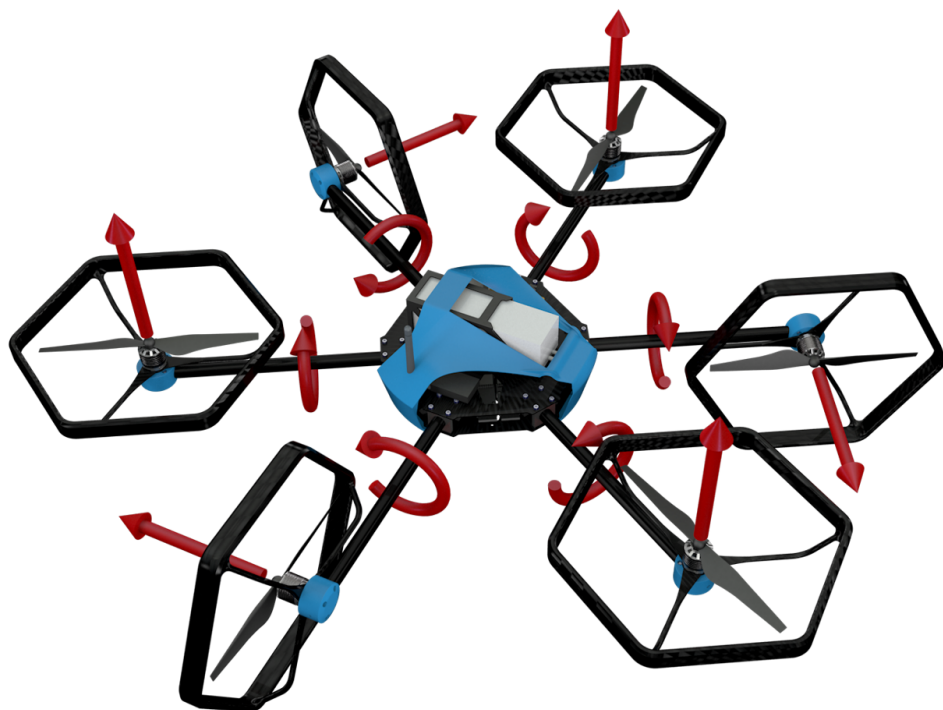
[In Copyright - Non-Commercial Use Permitted](#) →

This page was generated automatically upon download from the [ETH Zurich Research Collection](#). For more information please consult the [Terms of use](#).

Bachelor Thesis

Control Allocation of a Tilting Rotor Hexacopter

Spring Term 2017



Declaration of Originality

I hereby declare that the written work I have submitted entitled
Control Allocation of a Tilting Rotor Hexacopter
is original work which I alone have authored and which is written in my own words.¹

Author

Omar Elkhattib

Student supervisors

Marija Popovic
Mina Fekry Kamel

Supervising lecturer

Roland Siegwart

With the signature I declare that I have been informed regarding normal academic citation rules and that I have read and understood the information on 'Citation etiquette'.² The citation conventions usual to the discipline in question here have been respected.

The above written work may be tested electronically for plagiarism.

Place and date

Signature

¹ Co-authored work: The signatures of all authors are required. Each signature attests to the originality of the entire piece of written work in its final form.

² (<https://www.ethz.ch/content/dam/ethz/main/education/rechtliches-abschluessel/leistungskontrollen/plagiarism-citationetiquette.pdf>).

Abstract

The "Voliro" system developed during a one-year student project at ETH Zurich, is a novel concept of a rotary-wing UAV, designed as a multicopter with a classical planar configuration, whereby the thrust motors can be tilted around their axes. This allows the system to decouple position and orientation as well as move omnidirectionally.

This bachelor thesis adapts the allocation method used within the project to tackle specific critical orientations for which the general method cannot stabilize the system. The proposed strategy was to identify all critical orientations, then utilize a switch mechanism to change the general allocation to a specialized one, which can stabilize the system.

This allocation strategy was tested for feasibility in simulation and experimentally validated on the real life system.

Preface

First and foremost, I would like to thank my fellow team members of focus project Voliro, without which this thesis could not be possible. It was a wonderful opportunity and a pleasure to work with them.

Special thanks to my supervisors, which were always eager to help, and provided valuable inputs to keep me motivated and on the right track.

In particular I would like to thank:

- Prof. Dr. Roland Siegwart, head of the Voliro project
- Marija Popovic and Mina Fekry Kamel, my thesis supervisors

Most importantly, I am very grateful to all the friends and family members who supported me during the project and are helping me to achieve my goals.

Contents

| | |
|--|------------|
| Abstract | iii |
| Preface | v |
| Symbols | ix |
| 1 Introduction | 1 |
| 1.1 Problem Formulation | 1 |
| 1.2 Related Work | 2 |
| 1.3 Thesis Outline | 3 |
| 2 System Description | 5 |
| 2.1 Hardware | 5 |
| 2.2 Electronics | 6 |
| 2.3 Control Structure | 6 |
| 2.4 System Model | 6 |
| 3 General Allocation | 9 |
| 3.1 Allocation Problem | 9 |
| 3.2 Coordinate Transformation | 10 |
| 3.3 Performance | 11 |
| 3.4 Discussion | 11 |
| 3.5 Singularity | 14 |
| 4 Approach | 17 |
| 4.1 Adapted Dynamic Allocation | 17 |
| 4.2 Detection of Critical Cases | 18 |
| 4.3 Switch Mechanism | 20 |
| 4.4 Generalization | 21 |
| 5 Results | 23 |
| 5.1 Simulation Results | 23 |
| 5.1.1 Transition from Horizontal to Vertical Orientation | 23 |
| 5.1.2 Rotation During Vertical Orientation | 24 |
| 5.2 Flight Experiment Results | 26 |
| 5.2.1 Real Life Setup | 26 |
| 5.2.2 Transition from Horizontal to Vertical Orientation | 27 |
| 6 Conclusion | 29 |
| Bibliography | 31 |

Symbols

Symbols

| | |
|----------------------|--|
| ϕ, θ, ψ | roll, pitch and yaw angle |
| b | gyroscope bias |
| Ω_m | 3-axis gyroscope measurement |
| x | position vector |
| q | unit quaternion |
| \mathcal{F}_I | inertial world fixed frame |
| \mathcal{F}_B | body fixed frame |
| \mathcal{F}_{R_i} | i-th rotor frame |
| C_{AB} | rotation matrix from frame B to A ($u^A = C_{AB} * u^B$) |
| α_i | i-th propeller tilting angle around $e_x^{R_i}$ |
| ω_i | i-th propeller angular velocity |
| r_i^B | position of i-th propeller in body frame |
| x_B^I | position of body in inertial frame |
| ω_B^B | angular velocity of body in body frame |
| F_i | force generated by i-th propeller |
| τ_i | moments generated by i-th propeller |
| \mathbf{F} | total force acting on the body's center of gravity |
| \mathbf{M} | total moments acting on the body's center of gravity |
| m | mass of the body |
| I | moment of inertia of the body in its frame |

Acronyms and Abbreviations

| | |
|-------------|---|
| Albatross | First Prototype |
| BEC | Battery eliminator circuit |
| CF | Carbon Fiber |
| Colibri | Third Prototype |
| EKF | Extended Kalman Filter |
| ESC | Electronic speed controller |
| ETH | Eidgenössische Technische Hochschule |
| FC | Flight controller |
| IDSC | Institute for Dynamic systems and Control |
| IMU | Inertial Measurement Unit |
| MIMO | Multiple Input Multiple Output |
| Mockingbird | Second Prototype |
| MPC | Model Predictive Control |

| | |
|-------|-------------------------------|
| PCB | Printed circuit board |
| PDB | Power distribution board |
| Props | Propellers |
| PWM | Pulse width modulated signal |
| RC | Radio Controlled |
| ROS | Robot Operating System |
| SISO | Single Input Single Output |
| UAV | Unmanned Aerial Vehicle |
| UKF | Unscented Kalman Filter |
| ZHDK | Zürcher Hochschule der Künste |

Chapter 1

Introduction

Throughout the past few years, the development and application of rotary wing UAVs has achieved great interest and progress. The growth of interest is due to the mechanical simplicity and reliability of such systems. They have applications in a large variety of sectors and continue to grow more popular and reliable for industry applications.

While they are becoming ubiquitous in emerging technologies, they possess a fundamental limitation in the way they move. If the multicopter needs to change its position, it needs to tilt its body in order to produce a force in the desired direction. The student project Voliro, supervised by the Autonomous Systems Lab at ETH Zurich, aimed to tackle this fundamental limitation by developing a system that can hover at any arbitrary orientations as well as change its position regardless of its current orientation. The system developed has six rotors arranged in a planar configuration as a regular hexacopter, but possesses the additional degree of freedom of tilting the individual rotors around their axes. This is possible due to tilting motors fixed inside of the axes. With this mechanism, the system can produce forces and moments in all directions, by orienting the rotors in the desired direction.

This design would allow even more applications of UAVs that require the system to hover at a different orientation than the horizontal one. Examples for such applications are bridge inspections or general infrastructure maintenance. This would normally require expensive and time consuming crane constructions that allow the user to apply measurements to the surface of the bridge. With this new system, the multicopter can adapt its orientation to a wall or any curved surface and even press against it, such that measurements with external sensors can be performed with ease.

1.1 Problem Formulation

The main problematic faced during the project was the successful allocation of the actuator inputs. Since the system uses 12 actuators to control the 6 degrees of freedom of space, there is a redundancy that must be solved. Furthermore, the 12 actuators are strongly coupled and extra measures have to be taken to obtain reasonable control inputs. The goal of this thesis is to find an allocation solution that stabilizes the system at all arbitrary orientations in space. This allocation method should also fulfill the constraints presented by the system hardware.

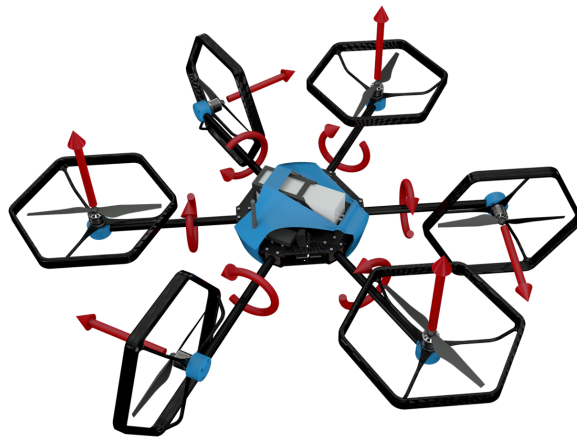


Figure 1.1: Representation of the twelve actuators of the system.

1.2 Related Work

Voliro's system is not the first system that fulfills the functionalities of omnidirectional flight. These can be summed up into two classes. The first being multicopters that can adapt their geometric configuration mid-flight using tilting mechanisms, while the second being multicopters that have rotors fixed at tilted angles such that forces and moments can still be produced in all directions. The following examples represent previous work in this field.

Quadrotor UAV with Tilting Propellers

A similar system with a tilting mechanism was conceptualized and experimentally tested¹ by Markus Ryll, which also uses tilting propellers to enable the decoupling of position and orientation. The system is based on a standard quadrotor configuration to allow efficient hovering in the horizontal orientation. The control scheme proposed with the system allows it to hover at a maximum pitch angle of 25°. Nonetheless, it proves the feasibility of a tilting rotor mechanism to control the six degrees of freedom in space independently.

Omnicopter

Also developed at ETH Zurich, the Omnicopter² of the IDSC is a system that can hover at all arbitrary orientations. Using an optimized geometric configuration of 8 fixed rotors, the system is capable of producing the same magnitude of forces and moments in all directions equally. To allow sufficient thrust in all directions, its motors can rotate around both directions. An extensive control strategy to utilize the decoupled position and orientation was implemented and verified in real life experiments.

Voliro's system builds upon the concept of tilting rotors, but can hover at larger arbitrary orientations, such as 90° or even 180°. The advantage of changing the geometric configuration mid-flight allows the system to adapt itself to stronger disturbances that would otherwise lead to actuator saturation.

¹Ryll, Bühlhoff, and Giordano 2013.

²Brescianini and D'Andrea 2016.

1.3 Thesis Outline

In chapter 2, a general description of Voliro's system will be given. Afterwards, chapter 3 explains the allocation problematic in more detail followed by the allocation solution used within the project. The performance of this solution is then discussed. Chapter 4 introduces an approach to adapt the general allocation such that the stability of the system can be improved in certain orientations. Finally, the results are demonstrated in chapter 5, followed by the conclusion and outlook to the thesis in chapter 6.

Chapter 2

System Description

As shortly described in the introduction, Voliro's system is a hexacopter with tilttable rotors. An insight into the hardware and electronics of the system will be given, followed by a general overview of the control structure and system model.

2.1 Hardware

The Voliro system¹ uses six thrust motors² and six tilting motors³ to allow itself to decouple position and orientation. The mechanism in place uses a shaft-to-hub connection from the tilting motor fixed inside the carbon tube with the thrust motor. This is facilitated by fixing the thrust motors around the axes via motor mountings directly connected with the tilting motors.

These axes are connected to the core, where the battery as well as the electronics required for flight, such as the electronic speed controllers and motion control boards for the tilting motors, can be safely stored.



Figure 2.1: The final prototype developed by Voliro, Colibri.

¹Voliro 2017.

²KDE2315XF-885

³Faulhaber 1226...B

2.2 Electronics

The electronics are a major part of the system's architecture. The most important component is the flight controller, the Pixhawk. This flight controller together with the open source software PX4⁴ allow the implementation of control algorithms on a microcontroller, which provides state estimation of the system, interfaces with the actuators and ultimately makes the system fly. This open source software provides a solid infrastructure for the control of UAVs as well as the capability of building upon it.

Due to the limited computational capacity of the microcontroller, an onboard computer⁵ was used to allow more complex algorithms to be used with the system. Furthermore, it enabled the communication with the system from a ground station, on which the user input software runs. A successful integration of onboard computer and flight controller was then facilitated.

2.3 Control Structure

The system is required to control all six degrees of freedom independently, and therefore a decoupled approach has to be taken with the control structure. The position and attitude control of the system are separated and treated individually. While the system has multiple inputs and multiple outputs, the different position coordinates and angles⁶, are treated as SISO systems, as it is assumed that the cross couplings between them are minimal.

The control structure used for both position and attitude is a cascaded loop of PID controllers, where the inner loop represents the linear velocities or angular rates, and the outer loop controls the absolute position and orientation of the system. This can be clearly seen in the following figure 2.2.

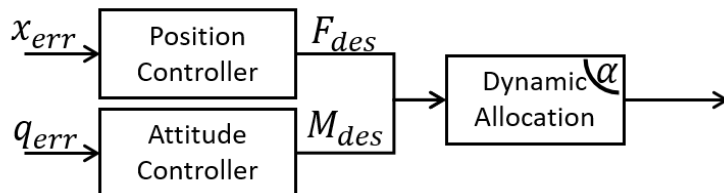


Figure 2.2: Schematic for the control structure for Voliro's system.

2.4 System Model

In order to tangibly describe the system, a set of coordinate frames was introduced. The two main frames are the fixed inertial frame, or the world frame, and the body frame of the system. The body frame mainly represents the current orientation of system, and is the frame in which the allocation occurs. Each individual tilting motor also has a coordinate frame, which describes the tilting angle relative to the body of the system.

⁴Meier, Honegger, and Pollefey 2015.

⁵Upboard

⁶Roll, pitch and yaw

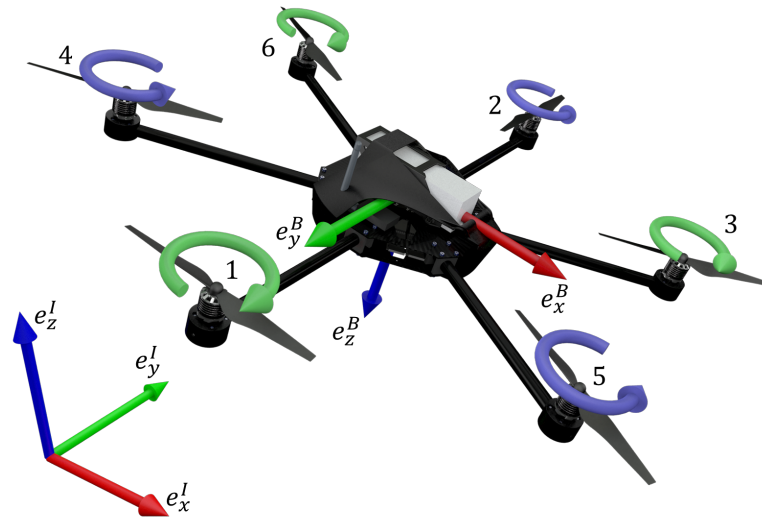


Figure 2.3: Illustration of the coordinate frames used to model Voliro’s system, where the rotors are numbered according to the HEXA X configuration used by the Pixhawk software.

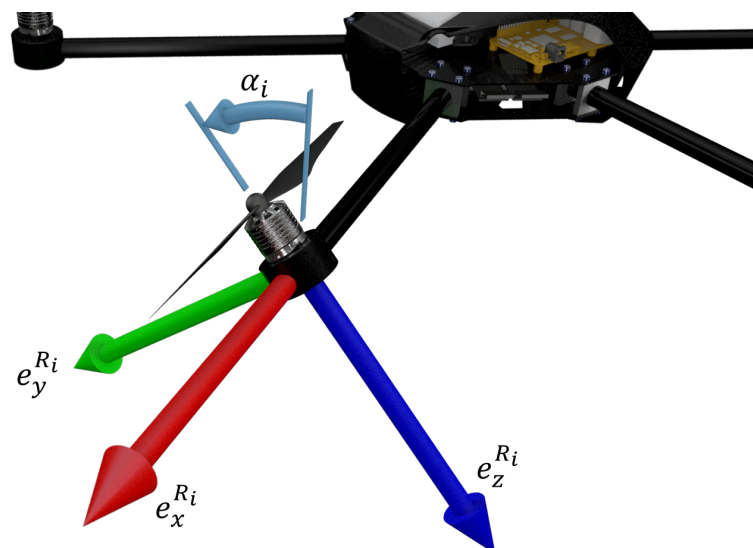


Figure 2.4: Coordinate frame of the rotor units.

Chapter 3

General Allocation

In the following chapter, the allocation problematic will be explained in more detail. Afterwards, the solution used within the Voliro project will be presented together with its performance. Finally, a discussion of this performance and necessary improvements will be done.

3.1 Allocation Problem

In order to allocate the control inputs for the the thrust and tilting motors, the allocation equation has to be derived. This equation 3.1 can be constructed by observing how the forces and moments provided by the combination of actuators act on the whole system, where the important matrix, \mathbf{A} , is called the allocation matrix.

$$\mathbf{A}(\boldsymbol{\alpha}) \cdot \mathbf{u} = \begin{pmatrix} F_{des} \\ M_{des} \end{pmatrix} \quad \mathbf{A} \in \mathbb{R}^{6 \times 6} \quad (3.1)$$

The allocation matrix of Voliro's system can be seen below.

$$\mathbf{A}(\boldsymbol{\alpha}) = \begin{pmatrix} -\mu s_1 & \mu s_2 & \mu \frac{1}{2} s_3 & -\mu \frac{1}{2} s_4 & -\mu \frac{1}{2} s_5 & \mu \frac{1}{2} s_6 \\ 0 & 0 & \mu \frac{\sqrt{3}}{2} s_3 & -\mu \frac{\sqrt{3}}{2} s_4 & \mu \frac{\sqrt{3}}{2} s_5 & -\mu \frac{\sqrt{3}}{2} s_6 \\ -\mu c_1 & -\mu c_2 & -\mu c_3 & -\mu c_4 & -\mu c_5 & -\mu c_6 \\ -\mu l c_1 - \kappa s_1 & \mu l c_2 - \kappa s_2 & \mu l \frac{1}{2} c_3 + \kappa \frac{1}{2} s_3 & -\mu l \frac{1}{2} c_4 + \kappa \frac{1}{2} s_4 & -\mu l \frac{1}{2} c_5 + \kappa \frac{1}{2} s_5 & \mu l \frac{1}{2} c_6 + \kappa \frac{1}{2} s_6 \\ 0 & 0 & \mu l \frac{\sqrt{3}}{2} c_3 + \kappa \frac{\sqrt{3}}{2} s_3 & -\mu l \frac{\sqrt{3}}{2} c_4 + \kappa \frac{\sqrt{3}}{2} s_4 & \mu l \frac{\sqrt{3}}{2} c_5 - \kappa \frac{\sqrt{3}}{2} s_5 & -\mu l \frac{\sqrt{3}}{2} c_6 - \kappa \frac{\sqrt{3}}{2} s_6 \\ \mu l s_1 - \kappa c_1 & \mu l s_2 + \kappa c_2 & \mu l s_3 - \kappa c_3 & \mu l s_4 + \kappa c_4 & \mu l s_5 + \kappa c_5 & \mu l s_6 - \kappa c_6 \end{pmatrix},$$

where $s_i = \sin(\alpha_i)$, $c_i = \cos(\alpha_i)$ and \mathbf{u} represents the vector of angular velocities.

$$\mathbf{u} = \begin{pmatrix} \omega_1 \cdot |\boldsymbol{\omega}_1| \\ \omega_2 \cdot |\boldsymbol{\omega}_2| \\ \omega_3 \cdot |\boldsymbol{\omega}_3| \\ \omega_4 \cdot |\boldsymbol{\omega}_4| \\ \omega_5 \cdot |\boldsymbol{\omega}_5| \\ \omega_6 \cdot |\boldsymbol{\omega}_6| \end{pmatrix} \quad \mathbf{u} \in \mathbb{R}^6 \quad (3.2)$$

The main problem here is the fact that the tilting angles $\boldsymbol{\alpha}$ and the angular velocities \mathbf{u} are strongly intertwined. They do not represent 12 linearly independent variables, instead they are coupled through this nonlinear allocation equation.

If the six tilting angles $\boldsymbol{\alpha}$ are predefined, there exists only one unique solution¹ for the angular velocities directly mapped by the allocation equation. This is due to

¹A system of linear equations with n linearly independent equations and n variables has only one unique solution.

the allocation matrix becoming constant. Once the tilting angles are known, there is no freedom to choose the angular velocities.

The problem with this is that the tilting angles have to be determined with the implications on the angular velocities in mind since the system has hardware constraints that must always be fulfilled. The motors must produce positive thrust under a specific maximum.

3.2 Coordinate Transformation

The allocation problematic could be heavily simplified using a coordinate transformation. The important quality of this coordinate transformation is that it bypasses the structure of previous solutions. Instead of allocating the tilting angles beforehand using the desired forces and moments, and then being forced to directly map the angular velocities, this coordinate transformation enables the simultaneous mapping of the tilting angles and the angular velocities.

To find this key coordinate transformation, the first observation was to notice that the allocation matrix can be constructed out of 6 independent columns that only contain the information of a respective rotor, 3.3. This means that there are no cross coupled terms between different α and ω . Secondly, the terms of the tilting angles are always sine or cosine of the respective angle, which appear linearly.

$$\mathbf{A} = [v(\alpha_1) \quad v(\alpha_2) \quad \dots \quad v(\alpha_6)] \quad (3.3)$$

When coupling the $\sin(\alpha)$ and $\cos(\alpha)$ terms with their respective ω as seen here 3.4, the allocation matrix can be transformed into one that is always constant 3.6, where the information of all 12 actuators is in the new solution vector \mathbf{x} . This new form of the allocation equation is similar to that of a regular multicopter.

$$x_{ci} = \cos(\alpha_i) \cdot \omega_i^2 \quad x_{si} = \sin(\alpha_i) \cdot \omega_i^2 \quad (3.4)$$

$$\mathbf{x} = [x_{c1} \ x_{s1} \ x_{c2} \ x_{s2} \ \dots \ x_{c6} \ x_{s6}] \quad \mathbf{x} \in \mathbb{R}^{12} \quad (3.5)$$

$$\mathbf{A}(\alpha) \cdot \mathbf{u} = \begin{pmatrix} F_{des} \\ M_{des} \end{pmatrix} \Rightarrow \hat{\mathbf{A}} \cdot \mathbf{x} = \begin{pmatrix} F_{des} \\ M_{des} \end{pmatrix} \quad (3.6)$$

The information of the tilting angles and angular velocities can then be obtained using the following equations, 3.8. The square root in the angular velocity term represents an implicit benefit of this solution, namely that the angular velocities are always positive. This is a noteworthy result because it guarantees the fulfillment of one of the hardware constraints of Voliro's system. There is, however, no guarantee for the second hardware constraint, that the maximum thrust of each rotor is not exceeded.

$$\mathbf{x} = \hat{\mathbf{A}}^\dagger \cdot \begin{pmatrix} F_{des} \\ M_{des} \end{pmatrix} \quad (3.7)$$

$$\alpha_i = \text{atan2}(x_{si}, x_{ci}) \quad \omega_i = \sqrt{x_{ci}^2 + x_{si}^2} \quad (3.8)$$

3.3 Performance

In the following section, the performance of this allocation solution will be investigated with a MATLAB simulation. The following plot 3.1 represents the overall position and orientation tracking behavior. After hovering for 10 s, the first input to the system is a setpoint of 60° in roll. In about 7 s the body roll angle converges to the desired 60° and is able to sustain this orientation. During this transition both the position and the pitch and yaw angles of the system remain around their desired values. The transition to 60° roll results in a smooth course of all angular velocities 3.2, which can also be observed in the curves of the tilting angles 3.3.

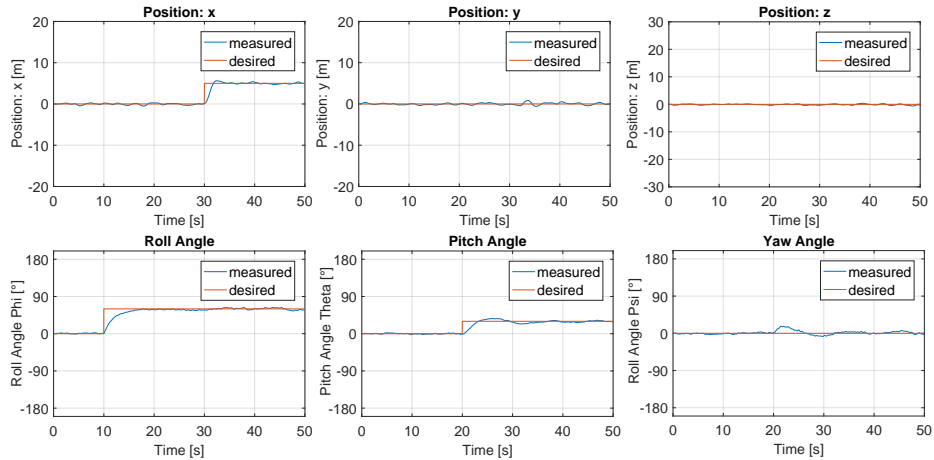


Figure 3.1: Step response for a combination of 60° roll and 30° pitch.

At 20 s, another desired orientation is given, 30° in pitch, which exhibits slightly different behavior. The change in pitch orientation of the system leads to a deviation of the yaw angle due to the cross couplings between pitch and yaw². The system can, nonetheless, quickly stabilize itself and reduce the orientation error back to 0° . The last reference input to the system is a step of 5 m in x direction at 30 s. In order to accomplish this, the allocation tilts the rotors 1 and 2 about 70° such that their thrust vector points directly in the x direction 3.3. Once the desired position is reached, the tilting angles return to their previous value for the system to hover.

3.4 Discussion

Overall, this allocation solution yields great results that can stabilize the system at arbitrary combinations of roll, pitch and yaw. The allocated tilting angles and angular velocities follow smooth courses regardless of disturbances. Additionally, the maximum achievable thrust of about 9.5 N is not exceeded even though this could not be guaranteed beforehand.

²Since these cross couplings have a small magnitude, the three orientation angles (roll, pitch and yaw) were treated as three separate SISO systems.

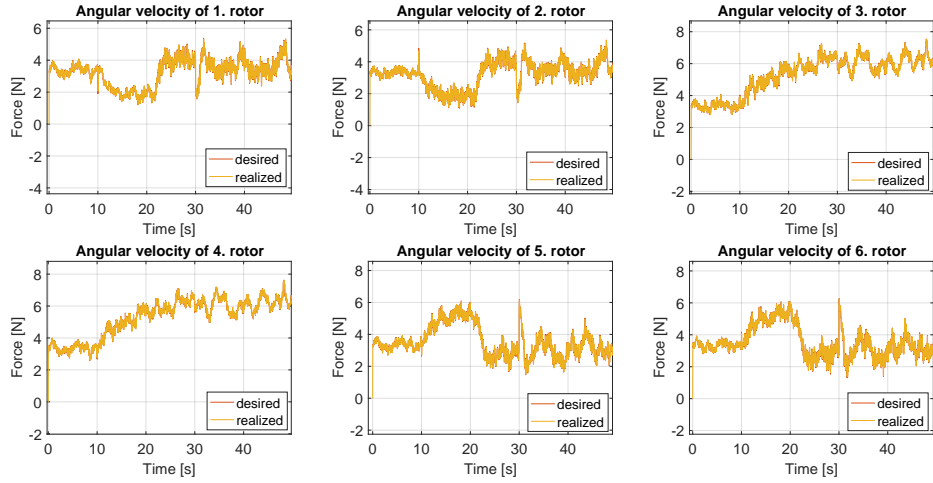


Figure 3.2: Angular velocities of all six motors for arbitrary position and orientation setpoints.

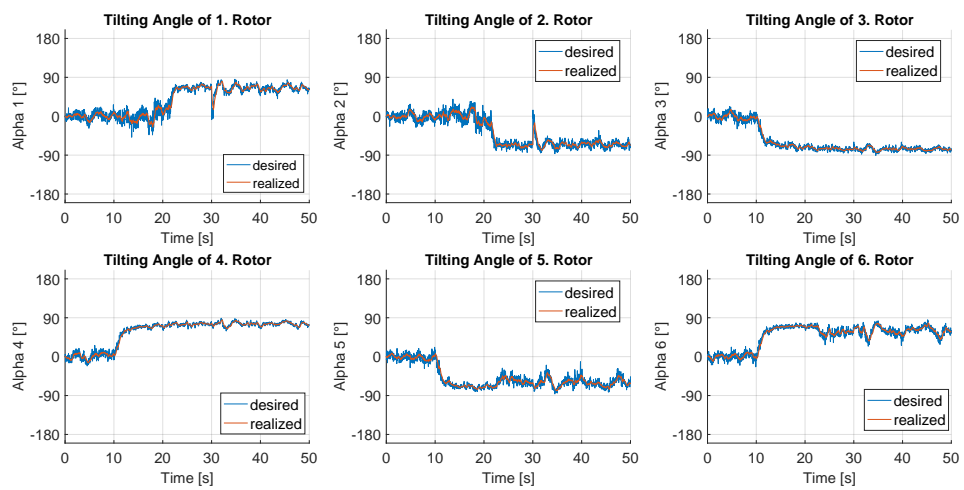


Figure 3.3: Tilting angles of all six motors for arbitrary position and orientation setpoints.

The efficacy of this solution is a result of the following important characteristics. First of all, this coordinate transformation resembles a transformation from Cartesian to Polar coordinates. The thrust vector³ of each individual rotor can be seen as the radial coordinate, while the tilting angle is the angular coordinate. The $\sin(\alpha)$ and $\cos(\alpha)$ terms appearing in the allocation matrix represent projections of the thrust vectors of the rotors onto the x-y plane as well as the z-axis of the body frame.

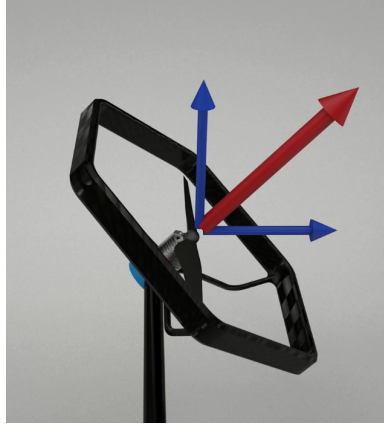


Figure 3.4: Projections of thrust vector

Given a desired force vector, this allocation solution rotates the thrust vector of each rotor such that it points to the desired direction as much as possible. Or mathematically speaking, the scalar product of a rotor thrust vector with the desired force vector should be maximized. The thrust is then distributed such that the rotors with a larger projection onto the desired force vector provide more thrust. The allocation has two degrees of freedom to accomplish this, the angle and the magnitude of the thrust, and assumes that they are always given as well as feasible. The tilting angle is determined with respect to maximizing the scalar product mentioned above, while the angular velocity is more involved.

A subtle advantage of using a pseudoinverse to solve for the vector \mathbf{x} is that it performs an optimization. Since the matrix $\hat{\mathbf{A}}$ has linearly independent rows, the Moore-Penrose pseudoinverse performs a least norm optimization⁴ of the solution vector \mathbf{x} . This minimizes the Euclidean norm of \mathbf{x} and has important implications. The \mathbf{x} vector is filled with the $\sin(\alpha) \cdot \omega^2$ and $\cos(\alpha) \cdot \omega^2$ terms, which when squared and added together give back ω^4 terms.

$$\|\mathbf{x}\|^2 = \sum_{i=1}^6 x_{ci}^2 + x_{si}^2 = \sum_{i=1}^6 \omega_i^4 \quad (3.9)$$

The squared norm of the solution vector is a summation of the angular velocities to the 4th power, 3.9, which represents the energy used by the system. Therefore, the pseudoinverse minimizes the energy of the system, by allocating larger angular velocities to the rotors capable of producing more thrust in the desired direction, while the others support with other required forces and moments. This explains how the overall thrust is distributed onto the rotors based on which ones are capable of providing larger desired forces and moments.

³Angular velocity vector

⁴Sprecher 2017.

3.5 Singularity

While this allocation solution generally yields good results, there are certain critical cases in which the allocation fails completely.

The allocation solution can stabilize the system at the vertical orientation of 90° pitch, when there are two rotors next to each other above the system. However, this is not the only configuration for the vertical orientation 3.5. When the system has one rotor directly above the system and another underneath it, such as with 90° roll, the system quickly goes unstable. This shows that the generality of the performance of this solution cannot be guaranteed.

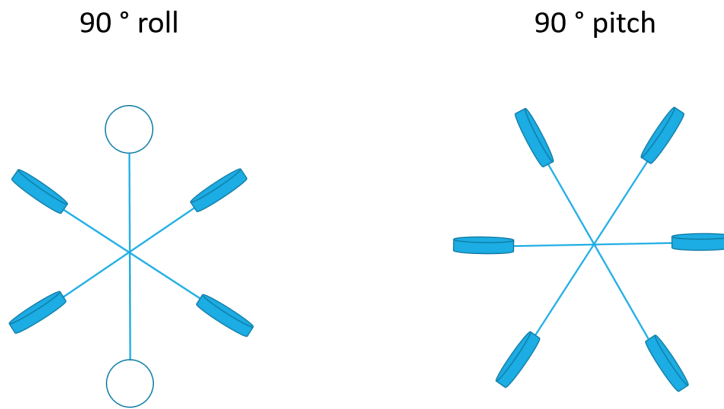


Figure 3.5: The two different configurations of the system in the vertical orientation.

The problem with this scenario is apparent when observing the tilting angles of rotors 1 and 2, the one at the top and the other at the bottom of the system. The respective tilting angles suddenly perform 180° revolutions back and forth or even continuously rotate around their axes, 3.6.

The behavior exhibited by the system at 90° roll can be explained in the following way. The rotors 1 and 2 can only provide forces in the inertial x-y plane or moments around the body x and the y axes. If the system should hold its position, the main objective of these rotors is to produce counteracting moments for the system. This requires the rotors to be able to produce them in both the positive and negative direction around the same axis. Due to disturbances and noise, the rotors will be required to constantly rotate over 180° back and forth to provide a force in the correct direction.

This behavior leads to gyroscopic effects, namely the motors producing a certain force while rotating to the next desired tilting angle, which are the primary cause of instability for the system. Additionally, the tilting motors used in the system have slow motor dynamics, which allows the gyroscopic effects to have a larger impact.

As such, a new solution that eliminates this irregular behavior of the tilting angles is required. The next step is to identify the critical cases that lead to this behavior and find an allocation solution that can maintain the stability of the system for them.

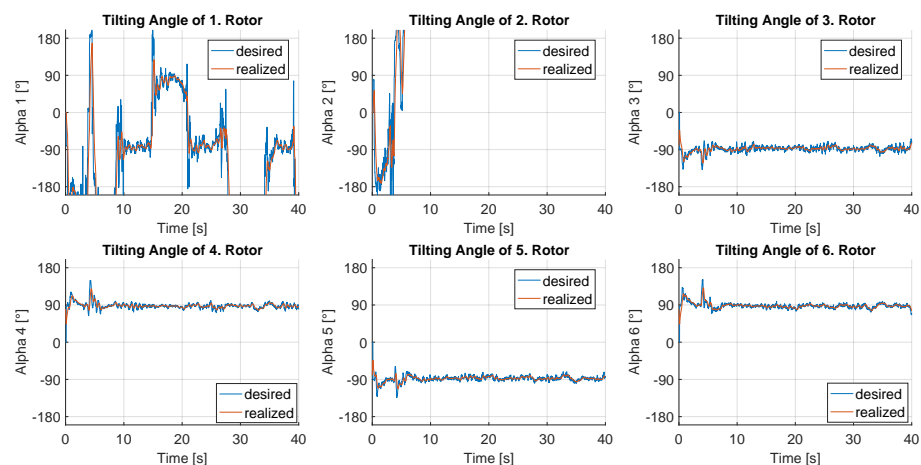


Figure 3.6: Instability of tilting angles at 90° roll.

Chapter 4

Approach

To allow the system to be stabilized in these critical orientations, an approach that adapts the existing allocation solution is investigated and presented.

Throughout this chapter, the general allocation solution discussed previously will be referred to as the *dynamic allocation* because the tilting angles are constantly changing.

The clear course to take is to remove the problematic tilting angles from the general allocation. One variant of this is to only remove the tilting angles, but use the angular velocities to have as much controllability as possible. Such an approach will be called a fixed angle allocation, and is briefly discussed here. Few approaches with this methodology were pursued, but the result was the same.

These approaches suffer from negative thrust requirements for the fixed rotors. Since these rotors only have one degree of freedom to produce forces and moments in the desired direction, the guarantee of positive thrust is no longer valid. This can be explained by the fact that the fixed rotors must be able to produce moments in both the positive and negative direction, as the allocation assumes all actuator inputs to be feasible. As a consequence, this leads to input saturation and the instability of the system. Thus, a new approach that avoids this problem was required.

4.1 Adapted Dynamic Allocation

The final approach was to adapt the dynamic allocation such that the advantages explained in 3.4 could be preserved, while the instability is prevented.

For the system to prevent negative thrust requirements, both the tilting angles and the angular velocities of the problematic rotors must be fixed¹. To perform this, their information has to be removed from the allocation matrix and the solution vector. This is accomplished by deleting their respective entries and therefore mapping the desired forces and moments only onto the four remaining rotors. As a result, the new solution vector contains 8 elements corresponding to the remaining four rotors.

The following example shows the allocation matrix and solution vector for the system without the rotors 1 and 2.

¹The tilting angles and angular velocities of the problematic rotors are set to 0

$$\hat{A}_{new} = \begin{pmatrix} 0 & \frac{1}{2}\mu & 0 & -\frac{1}{2}\mu & 0 & -\frac{1}{2}\mu & 0 & \frac{1}{2}\mu \\ 0 & \frac{\sqrt{3}}{2}\mu & 0 & -\frac{\sqrt{3}}{2}\mu & 0 & \frac{\sqrt{3}}{2}\mu & 0 & -\frac{\sqrt{3}}{2}\mu \\ -\mu & 0 & -\mu & 0 & -\mu & 0 & -\mu & 0 \\ \frac{1}{2}l\mu & \frac{1}{2}\kappa & -\frac{1}{2}l\mu & \frac{1}{2}\kappa & -\frac{1}{2}l\mu & \frac{1}{2}\kappa & \frac{1}{2}l\mu & \frac{1}{2}\kappa \\ \frac{\sqrt{3}}{2}l\mu & \frac{\sqrt{3}}{2}\kappa & -\frac{\sqrt{3}}{2}l\mu & \frac{\sqrt{3}}{2}\kappa & \frac{\sqrt{3}}{2}l\mu & -\frac{\sqrt{3}}{2}\kappa & -\frac{\sqrt{3}}{2}l\mu & -\frac{\sqrt{3}}{2}\kappa \\ -\kappa & l\mu & \kappa & l\mu & \kappa & l\mu & -\kappa & l\mu \end{pmatrix}, \quad \hat{A}_{new} \in \mathbb{R}^{6 \times 8}$$

$$\mathbf{x}_{new} = [x_{c3} \ x_{s3} \ x_{c4} \ x_{s4} \dots \ x_{c6} \ x_{s6}] \quad \mathbf{x}_{new} \in \mathbb{R}^8$$

4.2 Detection of Critical Cases

Now that the special allocation exists, the next step was to determine when the system enters a critical case in order to switch into the correct allocation.

The primary characterization of the critical cases is that there is one rotor directly at the top and another at the bottom of the system. If the vector between the center of mass and these two rotors in the inertial frame is observed, it can be seen that their z coordinates are substantially larger than those of the other four motors. Using this z coordinate, the critical cases can be identified.

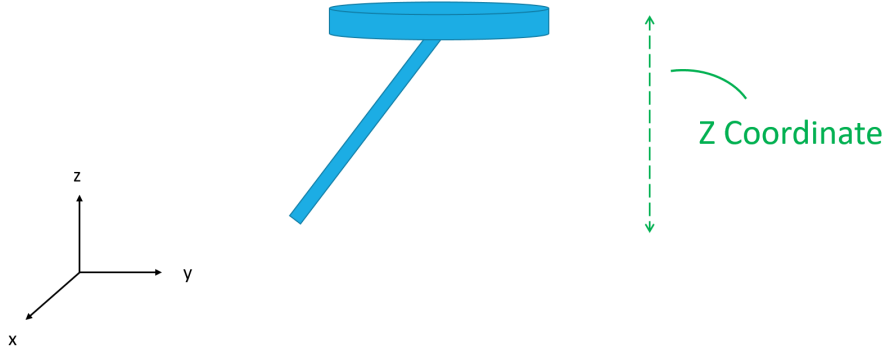


Figure 4.1: Detection of critical case.

However, there are two distinct switch cases that have to be dealt with. This first switch case only represents the transitioning of the system from the horizontal to the vertical orientation. Nearing the vertical orientation, the problematic rotors start exhibiting the undesired behavior of oscillating 180° around their axes.

The second case is when the system is already vertical, then rotates around the body z axis as seen in the following figure 4.2. As soon as the system deviates from this fully vertical orientation, two of the four motors stabilizing the drone are under substantially more stress. This is due to the two other motors being too inclined, such that they cannot contribute significantly to the hover thrust. As a result, the motors are required to produce infeasible thrust and are saturated, leading to a loss of altitude. The solution for this problem is to switch back to the general allocation faster than normal and use all six rotors to produce enough thrust.

To detect these two unique cases, the vectors of the individual rotors in the inertial frame were investigated. These vectors can be easily determined because their

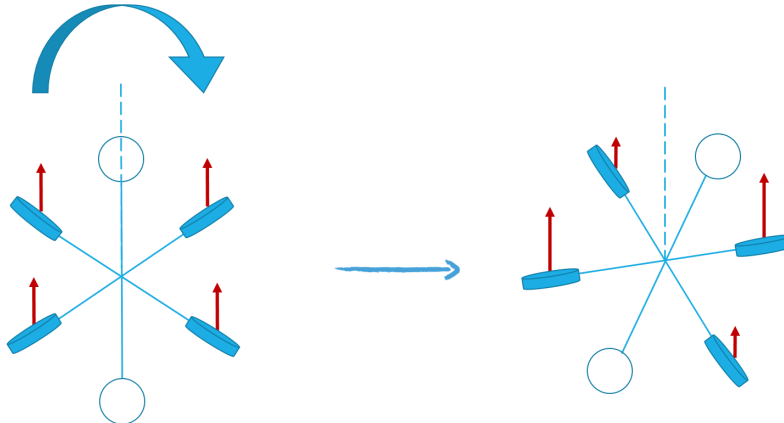


Figure 4.2: The second distinct switch case, rotating during vertical orientation.

coordinates in the body frame are known. They can then be transformed into the inertial frame using the rotation matrix representing the current orientation of the system.

For the first switch case, the important value is the z component of the vector. Taking the absolute value of the z component, two critical cases can be described, namely when the rotor is above or underneath the system. In both cases, the same pair of motors have to be switched off and thus the same special allocation has to be used.

To identify the second switch case, the xy component of the vector was observed. This component reflects a deviation from the vertical orientation and changes much faster than the z coordinate when the system is near the vertical orientation. It can therefore be used to switch back faster to the dynamic allocation. In the inertial frame, the x or the y coordinate cannot be looked at separately because if the system undergoes any yaw rotation, the coordinates no longer reflect the correct deviation.

There is, however, a clear problem with using the xy component, which is that it is strongly coupled with the z component. They are related through the following equation $x^2 + y^2 + z^2 = \ell^2$, where ℓ is the arm length. Since the two distinct switch cases have to be treated separately, this coupling significantly complicates the detection logic.

The main issue is that the switch using the xy component can only be done once the system is at or near the vertical orientation. To guarantee this, the z component and the xy component have to be assessed simultaneously. The choice of thresholds is then nontrivial because the two components influence one another, leading to problems with the logic.

In order to decouple the criteria for the two switch cases, a coordinate transformation was introduced. This transforms the vector into a special coordinate frame, where a rotation around the body z axis corresponds only to a deviation along one axis. This new coordinate frame is placed at the same position of the inertial frame, but is rotated around the z axis such that regardless of the current orientation of

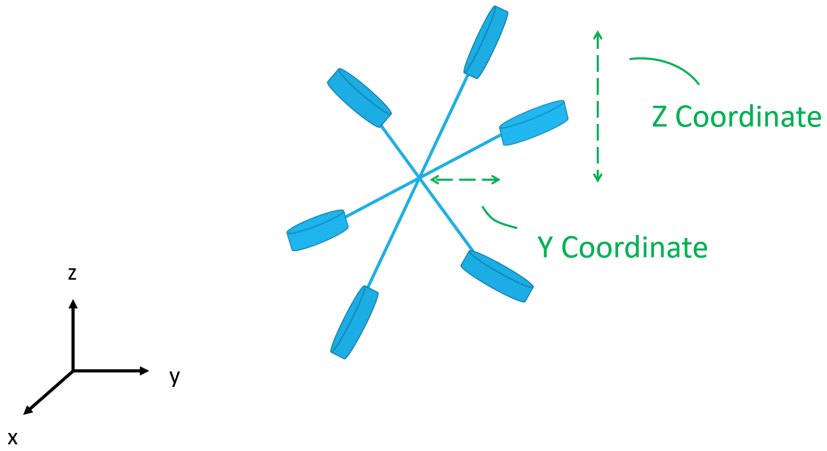


Figure 4.3: Criteria for critical case detection.

the system, a rotation around the body z axis always corresponds to a deviation in the y axis of the new frame.

What this means is that if the system performs any yaw rotation, the special inertial frame rotates with it. This way, the second switch case can be uniquely identified for all possible yaw angles of the system.

4.3 Switch Mechanism

The final step of this approach is the switch mechanism that decides which allocation the system should use. A significant problem that faces the system is constant switching back and forth between the different allocations due to noise and disturbances. To prevent this behavior, a hysteresis switch was implemented, which gives a buffer zone for the switching.

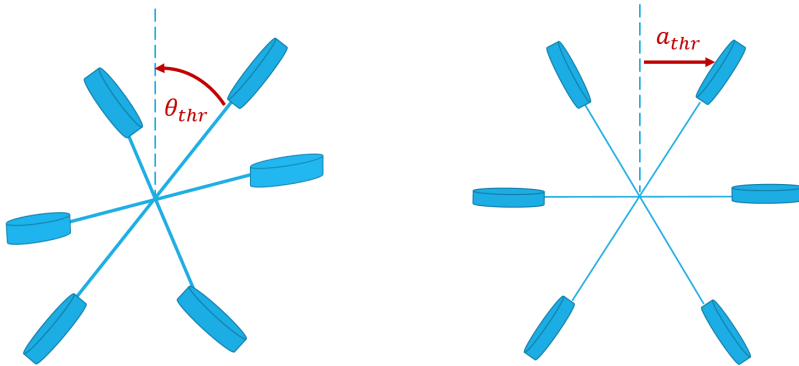


Figure 4.4: The two distinct switch cases.

There are two distinct hysteresis switches that represent the two switch cases. Each hysteresis requires an upper and lower bound threshold.

For the first switch case, θ_{ub} represents the switch from the general dynamic allocation to the special one, while θ_{lb} represents the other way around. The upper bound threshold θ_{ub} was determined to represent when the problematic rotors start rotating back and forth uncontrollably. The lower bound θ_{lb} was chosen as a trade-off between enough buffer room and quickly switching back to the general allocation to reduce the stress on the motors.

The second switch case does the opposite of the first one since the upper bound a_{ub} switches from the special allocation into the general dynamic one. For this case, the upper bound threshold a_{ub} exemplifies when two motors are overloaded and become saturated. Conversely, the lower bound a_{lb} is when the system is sufficiently close to the vertical orientation such that the undesired tilting behavior reoccurs.

4.4 Generalization

In this chapter, the three main tasks of the approach are presented for the case of the rotor pair 12. However, this single pair does not represent all possible critical cases. The same instability occurs when other rotor pairs are in the same vertical configuration, as seen in the following figure 4.5.

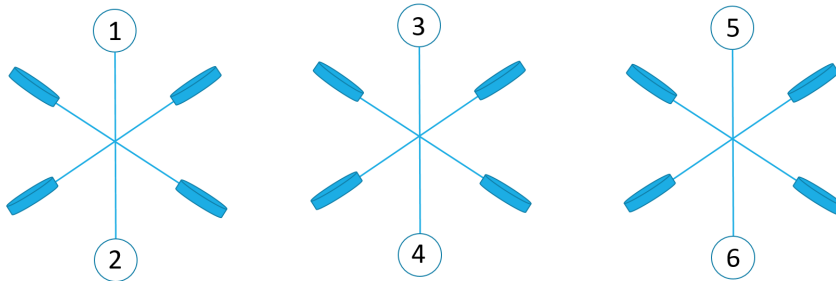


Figure 4.5: Critical configurations for different rotor pairs.

A clear advantage of this approach is that it can be easily generalized for the other rotor pairs of the system. The system has in total 3 distinct rotor pairs, for which a special allocation can be constructed using the same methodology in section 4.1. Besides this, a slight change to the detection has to be made. The coordinate transformation used to obtain the second switch criterion has to be adapted to correspond to a different rotor pair. This is done by an additional constant rotation around the inertial z axis.

Performing these changes, the generalized approach can be summarized as following. A high level case detection determines which pair of rotors is nearing a critical orientation. Once the pair is known, the switch mechanism for that rotor pair is activated. This is where the crossing of the thresholds is detected, and the system identifies the correct allocation for the respective situation.

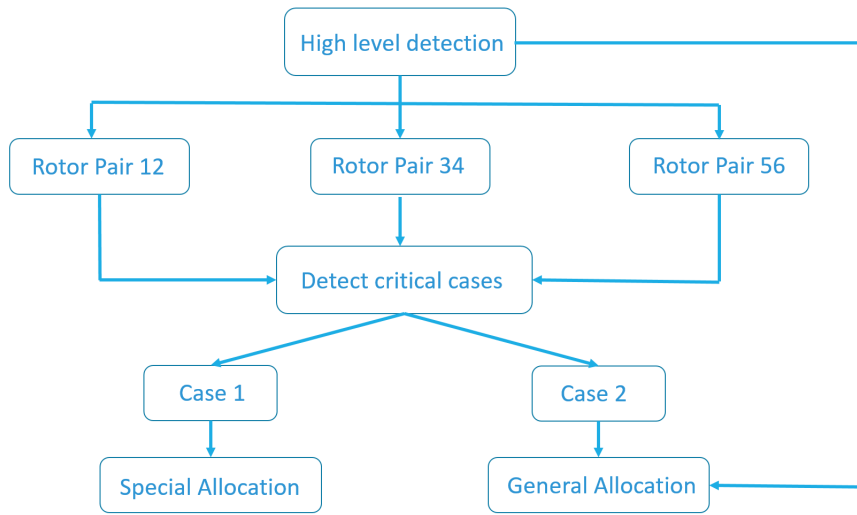


Figure 4.6: Illustration of generalized switch approach.

Chapter 5

Results

In this final chapter, a series of experiments will be conducted in both simulation and real life to evaluate the applied approach. The aim of the experiments is to test the two distinct switch cases used in the approach.

5.1 Simulation Results

After finalizing the approach, the next step was to validate its performance in simulation. The simulation experiments presented here are in Gazebo, which is an open source simulation environment with a physics engine that works with ROS¹. This physics engine models several important features such as gyroscopic effects and collision, which show the fidelity of the system.

An infrastructure that allows the PX4 software to be simulated in Gazebo was implemented within the focus project². This allowed a so-called software in the loop simulation, which was beneficial to test both the performance of the approach as well as the implemented software.

The hysteresis parameters were chosen as the following for the experiments:

$$\theta_{lb} = 68^\circ, \quad \theta_{ub} = 75^\circ, \quad a_{lb} = 3^\circ, \quad a_{ub} = 10^\circ$$

5.1.1 Transition from Horizontal to Vertical Orientation

The first simulation experiment conducted was the transition from the horizontal to the vertical orientation, 5.1. After hovering in the horizontal orientation for 10 s, the system slowly gets a setpoint to 90° roll. The roll angle is closely tracked by the system and at about 16s, the system is at 75° roll and successfully identifies the critical case. It then changes the allocation to the special one, where the problematic rotors, here 1 and 2, are switched off. This can be clearly seen from the plots of the angular velocities and tilting angles 5.2, as they are set to 0 as soon as the roll angle exceeds θ_{ub} .

The system transitions between the two different allocations successfully and is capable of stabilizing the system at 90° roll for 20 s. Although some deviations in the position occur, the system is capable of quickly reducing the tracking error. The system then starts the transition to the horizontal orientation, where the problematic rotors are switched back on as θ_{lb} is crossed.

¹Robot Operating System

²Voliro 2017.

This shows that the detection of the first switch case allows the system hover stably in the previously critical vertical orientation.

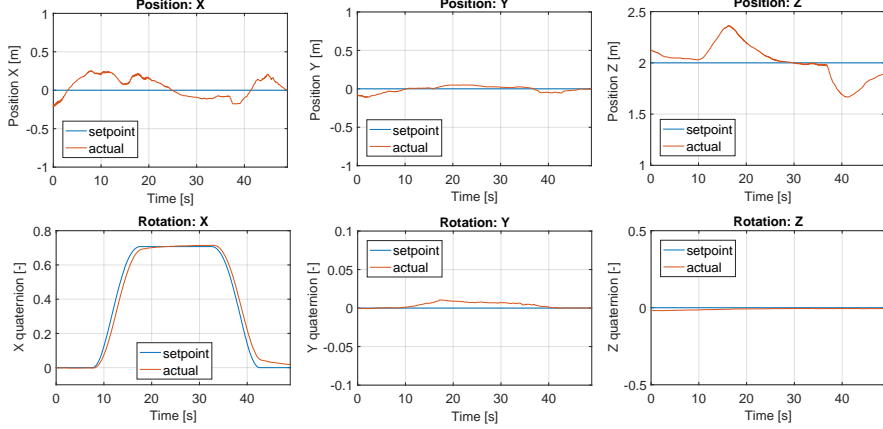


Figure 5.1: State of the system during transition from horizontal to vertical orientation.

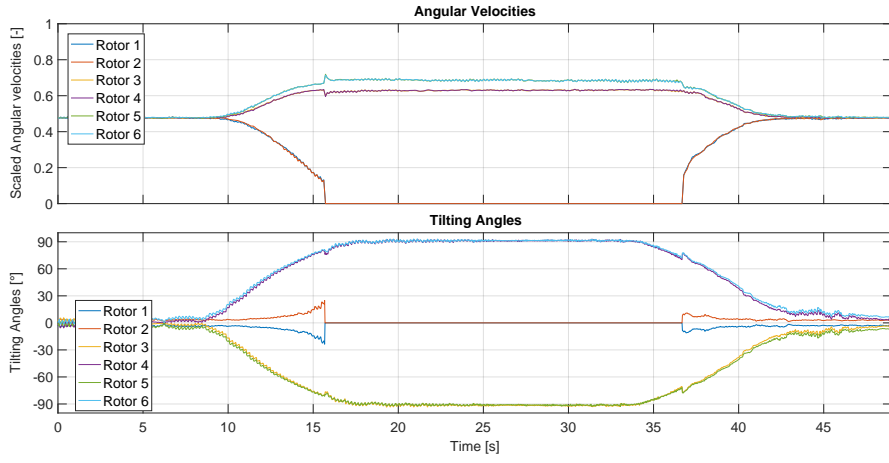


Figure 5.2: Angular velocities and tilting angles during transition from horizontal to vertical orientation.

5.1.2 Rotation During Vertical Orientation

A second experiment was conducted to test the other distinct switch case. The experiment starts with the system hovering at the vertical orientation of 90° roll. Afterwards, the system is required to rotate 15° around its body z axis 5.3. After

crossing the a_{ub} threshold of 10° , the previously unused tilting angles and angular velocities are switched back on to support the system while hovering. This can be seen by how the tilting angles 1 and 2 quickly rise to the desired 90° in the following figure 5.4. The system then rotates back to the vertical orientation and successfully switches to the special allocation. The process is repeated for a rotation of -15° , where the switch to the general dynamic allocation is also successful. Thus, the functionality of the detection and switch mechanisms have been validated by the simulation.

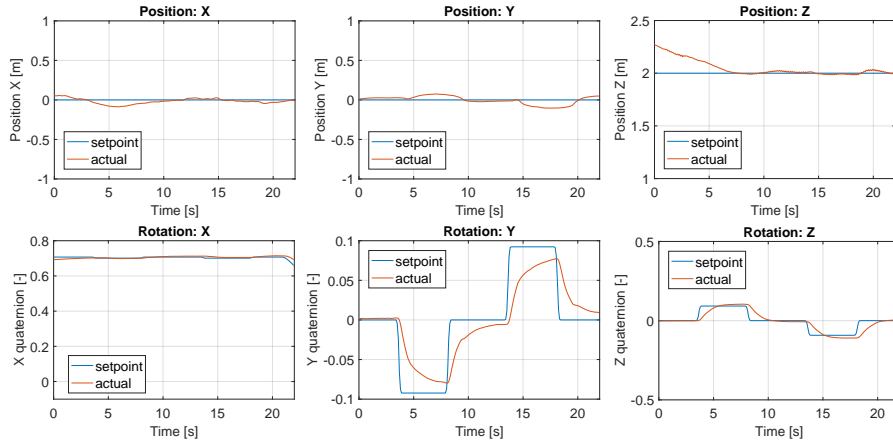


Figure 5.3: State of the system during rotation of 15° from vertical orientation.

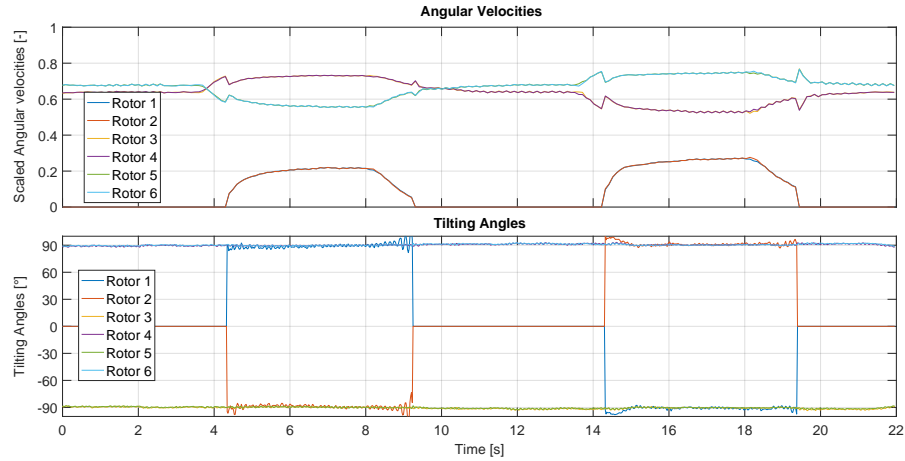


Figure 5.4: Angular velocities and tilting angles during rotation of 15° from vertical orientation.

5.2 Flight Experiment Results

The next step was to perform real life tests to allow a more valid evaluation. These tests provide a verification of the approach against model uncertainties, such as rotor thrust interference³. This is a parasitic effect that occurs when two rotors blow air into each other leading to a loss of produced thrust. The phenomenon occurs when the system is tilted at large angles and significantly affects the controllability.

5.2.1 Real Life Setup

There were a few steps to setup the experiment environment that will be shortly discussed here. After the approach was implemented using PX4, the algorithms were optimized due to the limited computational resources of the microcontroller.

For an accurate state estimation, an external motion capture system was used⁴. These accurate measurements were required for precise control of the system in the critical cases where the controllability was limited.

Additionally, since the maneuvers were performance critical, the system had to be secured to not crash into a wall or the ground. This setup is the same one used during Voliro's testing phase⁵.

This was performed by fixing the system with strings that restrict the flying space as well as prevent collision with the environment 5.5. Additionally, the floor was covered with mattresses to reduce the damage if in any case the system crashes into the ground.

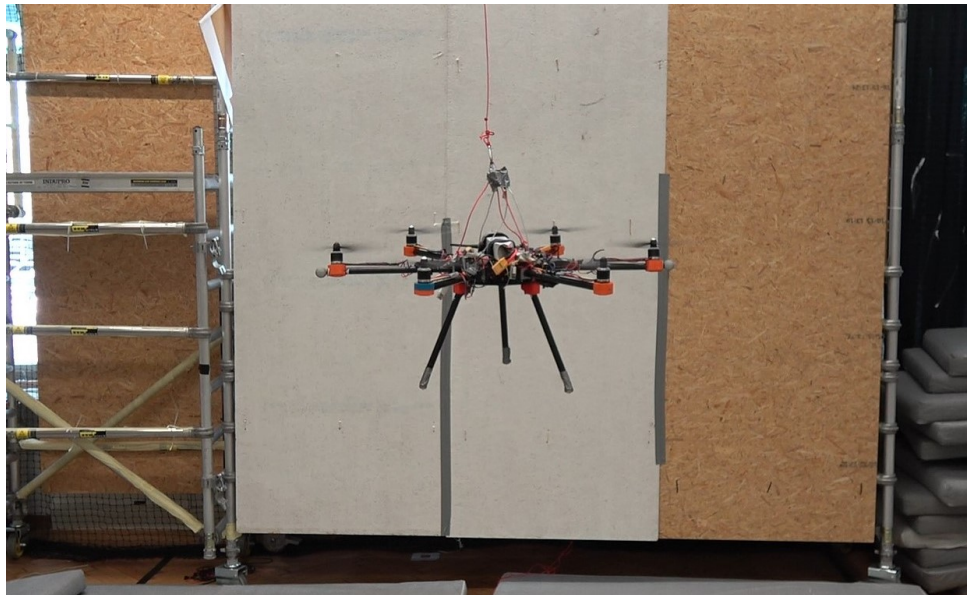


Figure 5.5: Illustration of system fixed with strings for a safe testing environment.

³This phenomenon is very difficult to model because Voliro's system experiences different degrees of thrust interference depending on the current orientation.

⁴Vicon Tracking System

⁵Voliro 2017.

5.2.2 Transition from Horizontal to Vertical Orientation

The same maneuver analyzed within the simulation was conducted in real life. The experiment begins with the system hovering. At the 20 s mark, the system starts the transition to the vertical orientation, 5.6, where the tracking of the roll angle is performed well. As the system crosses the switch threshold at about 27s, the critical case is correctly detected and the two rotors are completely switched off, 5.7. This time, however, the allocations are shortly switched back and forth as the roll angle oscillates around the lower bound threshold θ_{lb} . Shortly after, the system uses the special allocation as required and stabilizes the system at the critical orientation of 90° roll.

Contrary to the simulation, a clear cross coupling of the roll and pitch angle is now evident. Nearing the 90° roll angle, the system finds itself at 11° pitch. Larger deviations in the position are also present, especially for the z coordinate. This coordinate overshoots because of a feed forward term implemented to compensate for the rotor thrust interference.

Nonetheless, the system is capable of stabilizing itself briefly afterwards. The plot of the tilting angles 5.7 clearly shows how they are constantly changing to reject disturbances.

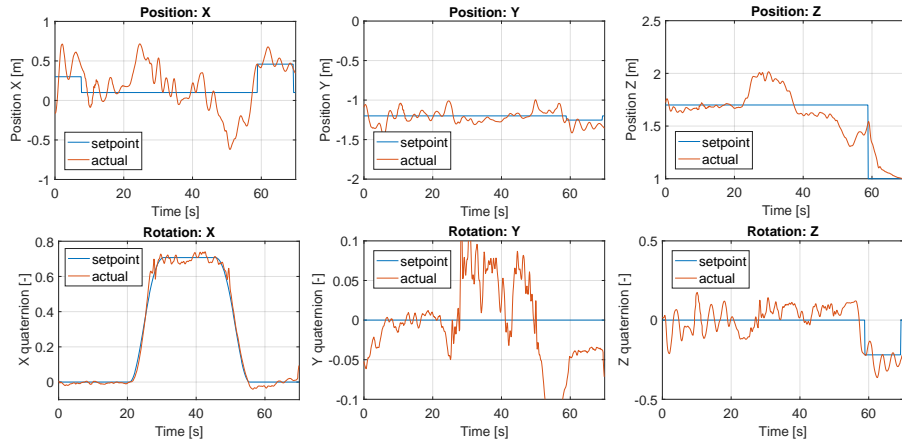


Figure 5.6: Real life experiment of horizontal to vertical transition.

It is noteworthy to mention that the angular velocities are extremely close or at the saturation limit at this configuration, as shown in figure 5.7. This explains how the system has trouble to quickly reduce the position and orientation errors.

After hovering at the vertical orientation for 20 s, the system transitions back to the horizontal orientation. Along the way, the switch to the general allocation is performed successfully.

Due to time constraints caused by the focus project, the second switch case could not be tested in real life. All in all, however, the system performs the same functionalities validated within the simulation. The experiment also shows the feasibility of the approach on a real life system.

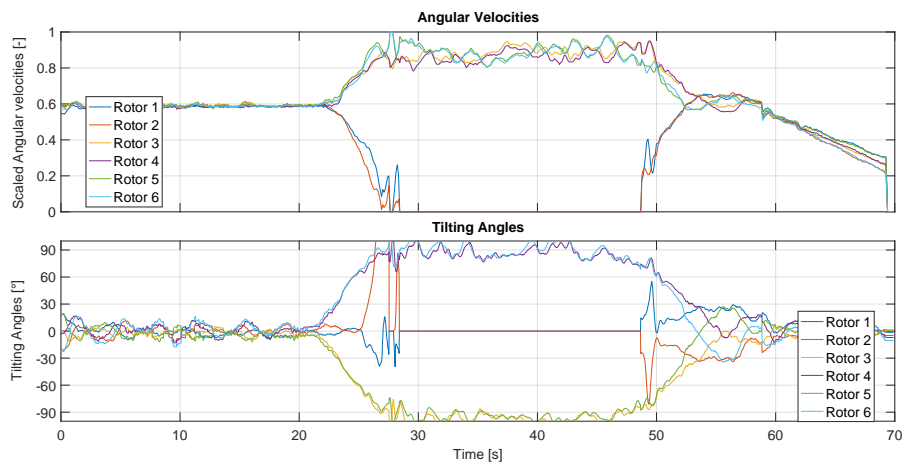


Figure 5.7: Angular velocities and tilting angles for real life horizontal to vertical transition.

Chapter 6

Conclusion

This bachelor thesis clearly demonstrates the theoretical and practical feasibility of a generalized allocation for the overactuated Voliro system.

An approach that allows the system to hover at previously critical orientations was proposed, which adapted the general allocation to detect the critical cases and then switch into a special allocation, with which the system is stable. It was shown that dealing with the critical cases guarantees the generality of the allocation.

This approach was then validated in simulation and tested in a real life environment, where the system successfully transitioned between allocations and hovered at the previously critical orientations. Additional experiments with the real life system to test the rotation from the vertical orientation were not conducted due to time constraints during the student project.

The performance of the approach can be improved further by tackling a few hardware problems, such as clearance in the tilting mechanism, which reduces the overall controllability of the system. Since the realized tilting angles can deviate from the desired ones by up to 20°, reducing this error would significantly boost the controllability and robustness of the system. To accomplish this, the shaft-to-hub connection of the tilting motor with the thrust motor could be designed to minimize the clearance. With these changes, the system would also be able to effectively counteract the rotor thrust interference occurring in the vertical orientation.

Future work could involve the problematic rotors to control the position of the system, where a more complex algorithm prevents them from oscillating when in the vicinity of the desired position.

In conclusion, the thesis confirms that Voliro's system can be stabilized when hovering at any possible orientation including vertical orientations. This would allow applications at or near curved surfaces such as inspections.

Bibliography

- Brescianini, Dario and Raffaello D’Andrea (2016). “Design, modeling and control of an omni-directional aerial vehicle”. In: *Robotics and Automation (ICRA), 2016 IEEE International Conference on*. IEEE, pp. 3261–3266.
- Meier, Lorenz, Dominik Honegger, and Marc Pollefeyts (2015). “PX4: A node-based multithreaded open source robotics framework for deeply embedded platforms”. In: *Robotics and Automation (ICRA), 2015 IEEE International Conference on*. IEEE, pp. 6235–6240.
- Ryll, Markus, Heinrich H Bülthoff, and Paolo Robuffo Giordano (2013). “First flight tests for a quadrotor UAV with tilting propellers”. In: *Robotics and Automation (ICRA), 2013 IEEE International Conference on*. IEEE, pp. 295–302.
- Sprecher, Christian (2017). “Weighted Allocation Maneuvers with a Tilting Rotor Hexacopter”. Bachelor Thesis, ETH Zurich.
- Voliro (2017). “An Omnidirectional Hexacopter”. Focus Project Final Report, ETH Zurich.

